CELL CYCLE
2017, VOL. 16, NO. 9, 841–851
http://dx.doi.org/10.1080/15384101.2017.1304328

Taylor & Francis
Taylor & Francis Group

REPORT

Efficient generation of functional Schwann cells from adipose-derived stem cells in defined conditions

Songtao Xie[a,*], Fan Lu[b,*], Juntao Han[a], Ke Tao[a], Hongtao Wang[a], Alfred Simental[c], Dahai Hu[a], and Hao Yang[d]

[a]Department of Burn Surgery, Xijing Hospital, Fourth Military Medical University, Xi'an PR China State Key Laboratory of Cancer Biology, Xijing Hospital Fourth Military Medical University, Xi'an, Shaanxi Province, China; [b]Department of Biochemistry and Molecular Biology, China State Key Laboratory of Cancer Biology, Fourth Military Medical University, Xi'an, Shaanxi Province, China; [c]Department of Otolaryngology-Head and Neck Surgery, Loma Linda University Medical Center, Loma Linda, CA, USA; [d]Translational Medicine Center, Hong Hui Hospital, Xi'an Jiaotong University, Xi'an, Shaanxi, China

ABSTRACT

Schwann cells (SCs) are hitherto regarded as the most promising candidates for viable cell-based therapy to peripheral nervous system (PNS) injuries or degenerative diseases. However, the extreme drawbacks of transplanting autologous SCs for clinical applications still represent a significant bottleneck in neural regenerative medicine, mainly owing to the need of sacrificing a functional nerve to generate autologous SCs and the nature of slow expansion of the SCs. Thus, it is of great importance to establish an alternative cell system for the generation of sufficient SCs. Here, we demonstrated that adipose-derived stem cells (ADSCs) of rat robustly give rise to morphological, phenotypic and functional SCs using an optimized protocol. After undergoing a 3-week *in vitro* differentiation, almost all of treated ADSCs exhibited spindle shaped morphology similar to genuine SCs and expressed SC markers GFAP and S100. Most importantly, apart from acquisition of SC antigenic and biochemical features, the ADSC-derived SCs were functionally identical to native SCs as they possess a potential ability to form myelin, and secret nerve growth factor (NGF), brain-derived neurotrophic factor (BDNF) and glia-derived neurotrophic factor (GDNF). The current study may provide an ideal strategy for harvesting sufficient SCs for cell-based treatment of various peripheral nerve injuries or disorders.

ARTICLE HISTORY
Received 17 November 2016
Revised 2 March 2017
Accepted 6 March 2017

KEYWORDS
adipose-derived stem cells; cell differentiation; myelination; peripheral nerve; Schwann cells

Introduction

Peripheral nerve injuries (PNI) or disorders resulting in sensorimotor function deficits usually have devastating effects on quality of life and bring a heavy economic burden for society.[1-4] Fortunately, Peripheral nerves possess an intrinsic regenerative capability predominantly due to the plasticity of SCs, and SCs are key regulators of the regeneration process by supporting and guiding outgrowing axon to reach the target of reinnervation.[5-8] Nonetheless, functional recovery following nerve injury, especially in the presence of peripheral gap, is often poor owing to a lack of sufficient native SCs in lesion. Based on these reasons, SCs were the first cells to be transplanted in microsurgery of nerve grafts, thereby improving nerve regeneration.[9-11] However, autologous nerve grafting resulting in honor site morbidity, the restricted mitotic activity and difficulties in harvesting limit deployment of SCs as describe cells.[12,13] Therefore, seeking alternative source of readily accessible and rapidly expandable cells would become a crucial.

A variety of stem cells including embryonic stem cells (ESCs) and induced pluripotent stem cells (iPSCs) can give rise to SC-like cells, which have functional behavior in both *in vitro* and *in vivo*.[14-19] However, the availability of the types of stem cells is extremely limited due to ethical consideration and risks of teratoma formation. Inspiringly, recent studies demonstrated that bone marrow mesenchymal stem cells (MSCs) can transdifferentiate into SCs like *in vitro*[20-22] and *in vivo*,[23,24] and are subject to none of these concerns. However, the difficulty in harvesting bone MSCs and relative low yield poses a major hurdle in their clinical applications.[25-28] Excitingly, ADSCs, as alternative MSCs, are able to self-renewal with differentiation multipotential, and have emerged as a more likely source for clinical use, owing to the ease of harvesting, higher yield, greater proliferation and immune-privileged potential.[26,28] Kingham et al showed that ADSCs could be converted into SC-like cells using a protocol similar to the method to induce bone MSCs.[25] The converted ADSCs acquired SC characteristics such as spindle shape, expression of SC markers, release of neurotrophic factors and myelin-forming potentials. Nevertheless, further improving the efficiency of differentiation of ADSCs into functional SCs should be developed.

In the present study, we attempted a combinational induction strategy to directly convert ADSCs into morphological, phenotypic and functional SCs. Using this protocol, we achieve 2 breakthroughs. First of all, we used olfactory ensheanthing cell conditioned medium (OECCM) in combination with several defined components to induce SCs to differentiate to SCs

CONTACT Dahai Hu hudhai@fmmu.edu.cn Department of Burn Surgery, Xijing Hospital, Fourth Military Medical University, Xi'an PR China State Key Laboratory of Cancer Biology, Xijing Hospital Fourth Military Medical University, Xi'an, Shaanxi Province, 710032, China; Hao Yang yanghao.71_99@yahoo.com Shaanxi Translational Medicine Center, Hong Hui Hospital, Xi'an Jiaotong University College of Medicine, Shaanxi China, 710054.
*These authors contributed equally to the work.
Color versions of one or more of the figures in the article can be found online at www.tandfonline.com/kccy.
© 2017 Taylor & Francis

without delivery of genes. Therefore, the conversion procedure is relative simple and safer. Secondly, the cell differentiation efficiency is high using the approach, by which can generate a great of amount of SCs. Of significance, SCs derived from ADSCs acquired physiology functions formation of myelination, release of neurotrophic factors. Therefore, the present study may provide a clue for the treatment of peripheral system injuries or diseases via autologous cell-based replacement.

Results

OECs characterization and identification

To prepare OEC conditioned culture medium for ADSC induction, we first cultured, characterized and identified OECs. Phase-contrast microscope showed that primary rat OECs exhibited unique morphology with polygonal or dipolar soma extending thin and long processes (Fig. 1). Notably, there are some round cells with with strong refractivity and stereoscopic perception on the upper of OECs and underlying large flattened cells. According to these cells morphology features, these cells may be contaminated cells such as degenerative OECs, microglial cells and fibroblasts (Fig. 1A). After purified and cultured for 5 and 7 days, almost all of cells show OEC morphological features. Non-OECs were hardly detachable under the culture conditions (Fig. 1B and C). To substantiate the purity of cultured OECs, purified OECs were subsequently stained by immunostaining with 2 specific markers P75 and GFAP for OECs. Immunocytochemistry showed that most cells in the culture system were intensely positive for P75 and GFAP (Fig. 1d-d″), suggesting that the induction culture medium is really produced from OECs.

ADSCs culture, purification and morphological features

Rat freshly isolated adipose cells for 3 d *in vitro* appeared as a monolayer of polygonal and flat squamous morphology without soma extensions (Fig. 2A). After culture of 7 days, almost of all exhibited large and flat fibroblast-like features and cytoplasmic extensions have formed whirl confluency (Fig. 2B). When purified ADSCs by flow cytometry were cultured for 3 days, the majority of cells show irregular and flat fibroblast-like morphology (Fig. 2C). Seven days later, these ADSCs reached confluency, displaying a parallel alignment (Fig. 2D). Flow cytometry analysis of rat ADSCs at 3 passages revealed that ADSCs were negative for CD31 and positive for CD90 (Fig. 2E and F). The percentage of $CD90^{+}$ cells was over 96.7%, suggesting that sorted and further passaged ASCs still keep high purity.

Identification and characterization of stem cell with ADSC properties

To determine whether subcultured ADSCs are genuine ADSCs, at passage 2, the characteristic marker (CD29, CD44, and CD90) expression of cells were further examined by immunofluorescence. As shown in Figure 3A-C, these passaged ADSCs showed positive for 3 specific markers and the percentage of positive is still high. Further, to confirm whether these cells at passage 2 still have mesenchymal stem cell properties, the ADSCs at passage 2 were induced differentiation to mesodermal lineage and further stained. The staining results showed that following the 3 different mesodermal differentiation, ADSCs were able to produced fat droplets, chondrocytes and osteocytes as 3 different signs of mesodermal differentiation occurred. Of note, Oil red O for fat droplets (Fig. 3D), Toluidine Blue for chondrocytes (Fig. 3E) and Alizarin red S for osteocytes (Fig. 3F). Normal ADSC staining was not shown for no staining was found.

Morphological changes following differentiation with different inductions

To screen the best approach for inducing conversion of ADSCs to SCs, We induced ADSCs with 4 different

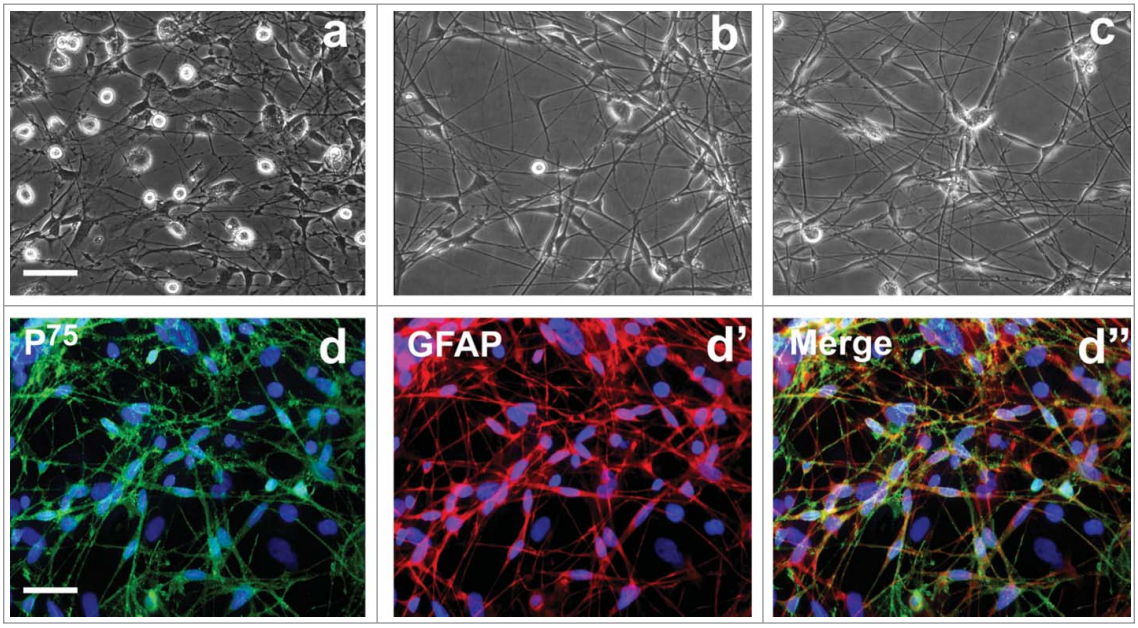

Figure 1. Morphological and biochemical properties of primary olfactory ensheathing cells. (A) Primary OECs at 7 d of culture. (B, C) Primary OECs after purification at 5 and 7 d in vitro. (d-d″) Immunostaining identification revealed expression of p75 and glial fibrillary acidic protein (GFAP). Scale bars = 100 μm.

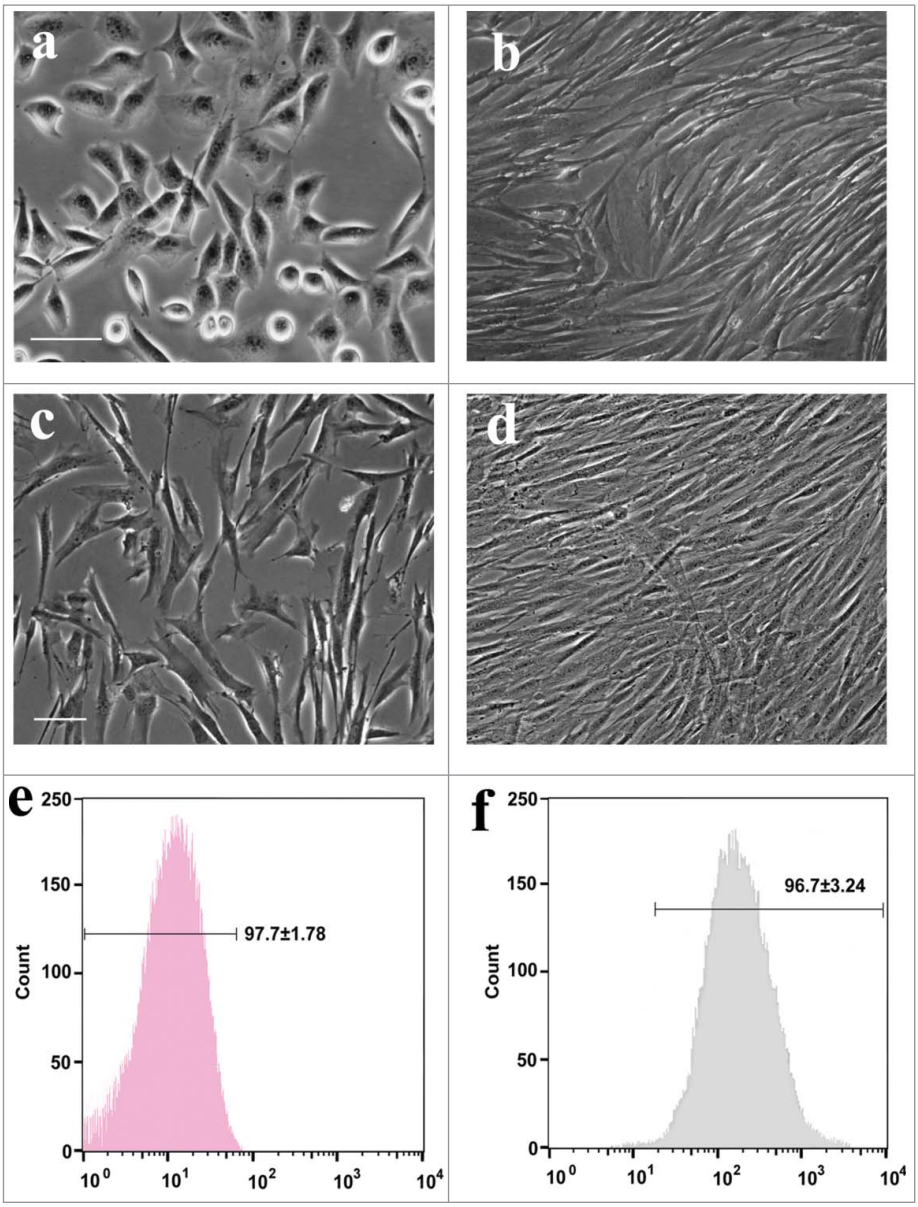

Figure 2. Phase-contrast images and flow cytometric ADSCs. (A, B) The morphology of primary ADSCs at 3 and 7 d in vitro, respectively. (C, D) Purified ADSCs at 2 and 5 d in vitro. (E, F) Rat ADSCs at 2 passages were harvested for flow cytometric analysis with CD31 and CD44.

differentiation conditions supplemented with or without OECCM, SB and retinoic acid (RA). Among these conditions, OECCM supplemented with several defined factors, including SB, forskolin (FSK), RA, β-mercaptoethanol (BME) and FGF was the best approach for inducing the conversion of ADSCs to SCs. As shown in Figure 4, morphological changes were first were observed to evidence the conversion of ADSCs to SCs. After the induction with OFRFS (combined with OECs, FSK, RA, FGF and serum), some cells changed into bipolar spindle-shape cells similar to native SCs. In addition, most cells in cultures still maintained their original squamous morphology and cell proliferation remarkably decreased (Fig. 4A). When cells were induced with OFFS or OSFRBFS, most cells changed to spindle-like morphology and the parallel aligned cells were clearly seen (Fig. 4B and C). When cells were treated SFRBFS, bipolar spindle-shape cells were hardly seen but some cells extend long processes. Similar to OFRFS group, most cells still kept original morphology (Fig. 4D). As for control group, no remarkable changes were found (Fig. 4E).

Morphological and phenotypic characterization of ADSCs during differentiation

Even though the earlier work performed morphological observation revealed that under different induction conditions, ADSCs can acquire SC-like morphology, it is unknown if these cells also possessed biochemical phenotype of SCs. Next, we characterized and identified the cells derived from ADSCs by specific marker expression and immunochemical phenotypes. Under several indicated inductions for 1 and 3 weeks, OECCM with chemicals SB, BME in conjunction with a variety of factors like FGF, RA, and FSK was the best protocol for inducing ADSCs to SCs.

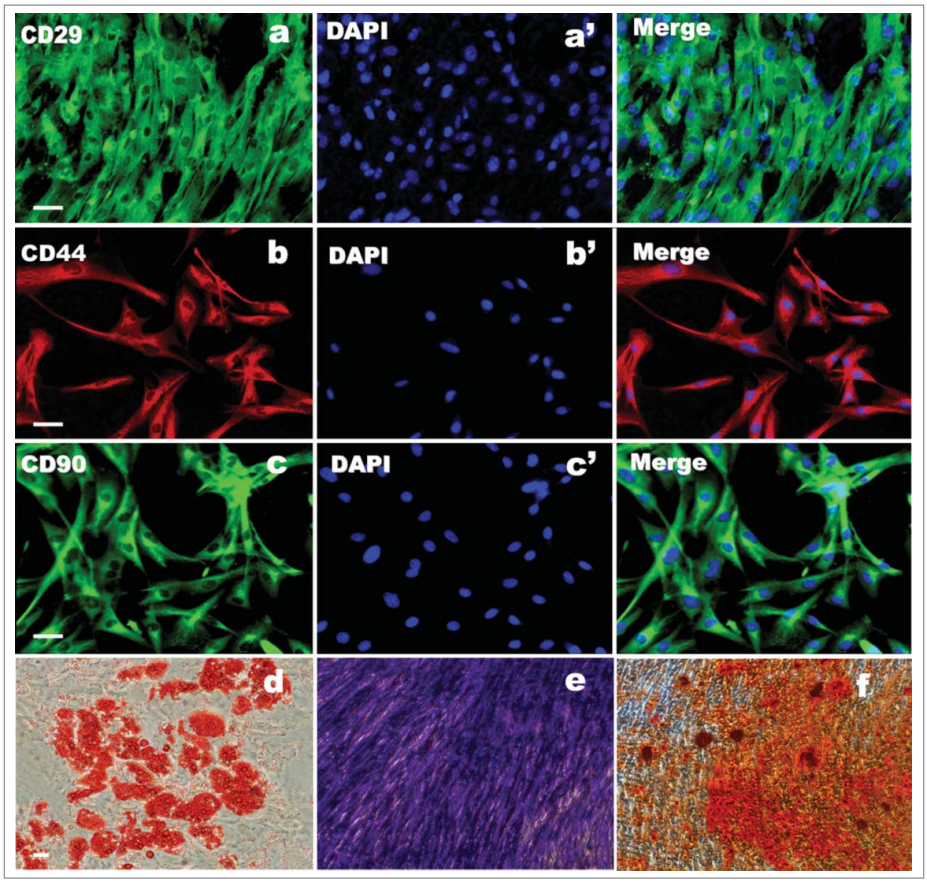

Figure 3. ADSC biochemical identification and evaluation of multipotency. (A, B, C) ADSCs immunostained positively for CD29, CD44, and CD90. (a′, b′, c′) DAPI staining. (D, E, F) Trilineage of differentiation of ADSC after induction of 21 d. (d) The results of adipocytic differentiation with fat droplet stained with Oil red. (E) Chondrogenic differentiation with proteoglycans stained with Toluidine blue. (F) Osteogenic differentiation with calcium deposits stained with Alizarin red Scale bars = 100 μm.

This was evidenced by drastic elevated expression of SC markers S100 and GFAP (Fig. 5A), albeit other inductions also initiated a remarkable increase in 2 molcule expression. Overall, there is a significant difference compared with other induction groups. Inspiringly, with prolongation of cell induction time, the 2 molcules all exhibited an increase tendency. In line with the gene expression, western blot analysis also showed a similar expression pattern at protein levels, thus further verified the OSFRBFS as the best protocol for inducing ADSC conversion (Fig. 5B). To substantiate

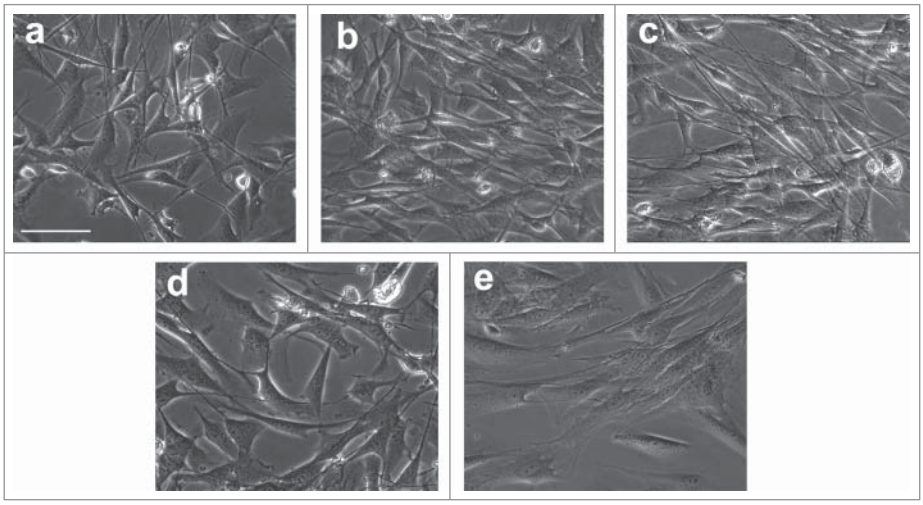

Figure 4. Morphological change of ADSCs during differentiation with different inductions. After a 2-weeks culture in the different induction mediums. ADSCs changed from squamous, flat fibroblast-like cells to spindle-shaped cells similar to genuine SCs. (A) ADSCs were induced with OFRFS (B, C) cells were induced with OFFS or OSFRBFS, most cells changed to spindle morphology and the parallel aligned cells were clearly seen. (D) Little bipolar spindle-shape cells were seen when induced with SFRBFS. (E) an image of culture from control group. OFRFS, a combination of OECCM, FSK, RA, FGF and serum; OFFS, a combination of OECCM, FSK, FGF and serum; OSFRBFS, a combination of OECCM,SB, FSK, RA, BME, FGF and serum; SFRBFS, a combination of SB, FSK, RA, BME, FGF and serum. Scale bars = 100 μm.

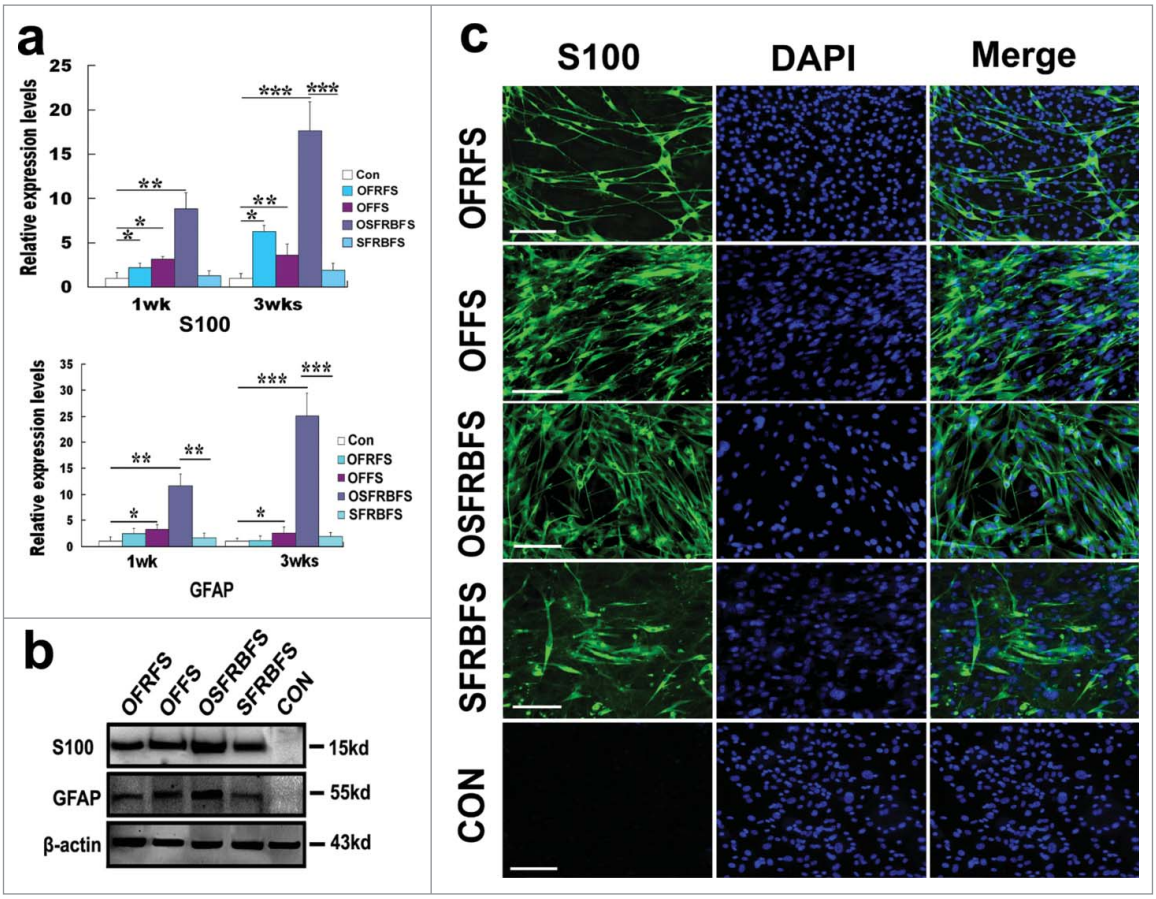

Figure 5. Biochemical and morphological characteristics of ADSCs induced in different medium compositions. (A) real-time polymerase chain reaction showed that mRNA levels of S100 and GFAP in ADSCs induced with OFRFS, OFFS, OSFRBFS and SFRBFS both for 1 and 3 weeks, respectively. Notably, the OSFRBFS most significantly increased the expression levels of the 2 molcules in ADSCs. All data are reported as mean ± SEM. $^{*}p < 0.05$ compared with the relevant controls; $^{**}p < 0.01$; and $^{**}p < 0.001$ (B) Western blots further support expression of the 2 molcules in ADSCs under the indicated conditions. β-action served as loading control of total protein. Strikingly, the expression levels of the 2 molcules in ADSCs with OSFRBFS induction showed the highest upregulation. (C) immunofluorescence revealed the upregulation of SC marker S100 in the cells derived from the ADSCs induced with the indicated conditions. Scale bars = 100 μm.

the assumption regarding this best approach for conversion of ADSCs to SCs, immunofluorescence was performed to characterize ADSC-derived differentiated cells. Strikingly, these distinct inductions can convert ADSCs into $S100^{+}$ cells but the difference in proportion of positive cells. Overall, from the representative photograph, the efficiency of ADSCs conversion appeared higher. But in comparison, the percentage of $S100^{+}$ cells is highest in OSFRBFS induction group (Fig. 5C).

High efficiency of the conversion of primary ADSCs to SCs

To substantiate the screened protocol as best approach for conversion of ADSCs to SCs, we further investigated the differentiation of ADSCs into SCs following OSFRBFS. As shown in Figure 6, after 1 to 3 weeks of induction, ADSCs gradually acquired SC biochemically phenotypic features, displaying a progressive increase in expression of S100 and GFAP at both gene and protein levels (Fig. 6A and B). Quantification analysis revealed that conversion of ADSCs was effectively enhanced by the best induction protocol (Fig. 6C). Furthermore, these induced ADSCs also progressively developed SC-like morphology, displaying dipolar and tipolar soma bearing thin and long processes. Also immunostaining analysis showed that these differentiated cells are positive for S100 and the proportion of $S100^{+}$ cells drastically increased within 3 weeks (Fig. 6D). Quantification revealed a significant increase in the $S100^{+}$percentage (ranging from 21.7 ± 3.5% to 89.5 ± 8.1% within 1–3 weeks), indicating that OSFRBFS was the optimal protocol for efficient conversion of ADSCs to SCs (Fig. 6E). In addition, to further confirm that the ADSCs-derived SCs from different passages could maintain high proliferative capacity, the converted cells were continually cultured at the indicated time points, and cell proliferation or viability was assessed by MTT assay. As shown in Figure 6F, there was a dramatic increase in cell proliferation capacity for each passage from 2 to 4 with prolongation of culture time, and the tendency of cell proliferation keep consistent. Moreover, no significant difference in cell proliferation was found among 3 different passages, which revealed that the converted cells can maintain same proliferation after subculture.

ADSCs-derived SCs could form myelin and release neurotrophic factors

To further investigate whether ADSCs-derived SCs are functional, we assessed myelin-forming ability of differentiated ADSCs and further determined release of neurotrophic factors

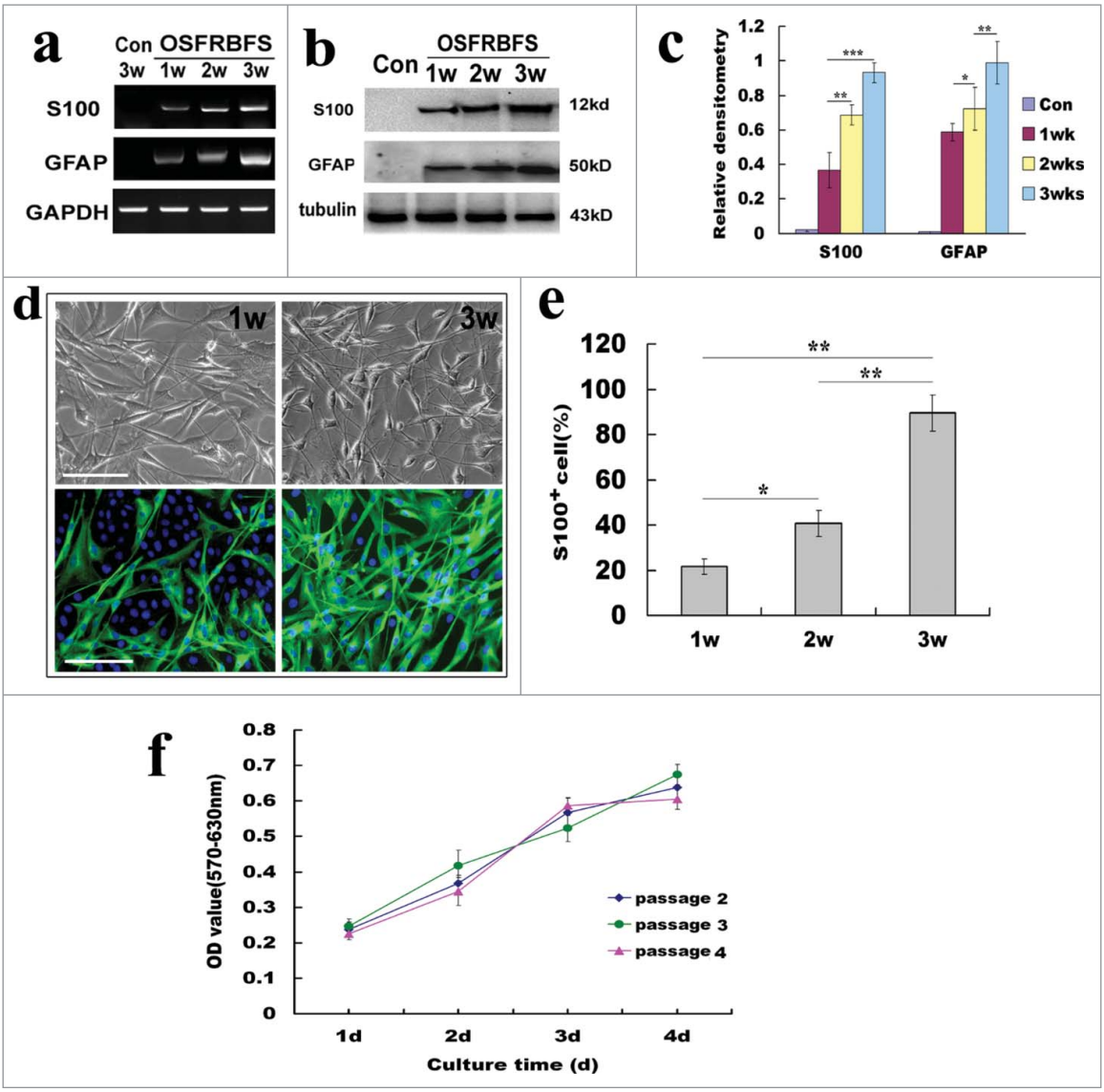

Figure 6. Optimal induction for efficiency of the conversion of ADSCs to SCs. (A, B) Reverse transcription PCR and western blots showed the changes of SC phenotypic markers S100 and GFAP at gene and protein levels under the optimal induction. GAPDH and β-Action served as loading control of RNA or total protein, respectively. (C) Quantification of SC marker expression during differentiation of ADSCs at different induction stages. Notably, the expression levels 2 molcules in ADSCs induced with OSFRBFS show a significant time-dependent upregulation. (D) Immunofluorescence images of differentiated ADSCs stained with S100 at 1–3 weeks. Notably, the images of induced ADSCs with OSFRBFS for 2 weeks were not shown because of no significant difference with 1 week. (E) Percentages of S100 positive cells after induction within 3 weeks. (F) The change of proliferative capacity of the convert cells from different passages with longer culture time. All data are reported as mean ± SEM. $^{*}p<0.05$ compared with the relevant controls; $^{**}p<0.01$; and $^{**}p<0.001$. Scale bars = 100 μm

NGF, BDNF, and GDNF in ADSCs-derived SCs. For assessment of myelin-forming, DRG neurons were co-cultured with ADSCs-derived SCs for 2 weeks. As shown in Figure 7A and B, after co-culture of DRG neurons with ADSCs-derived SCs for 12 days, many of differentiated ADSCs processes progressed along neuronal aligned axons, and even were wrapped at certain segments. Immunostaining also revealed that Tuj-1 was colocalized with BMP expression as indicative of myelin protein expression. To further substantiate that differentiated ADSCs can form functionally peripheral myelin, we also immunestained co-culture of dorsal root ganglion (DRG) and the differentiated ADSCs at low density with anti-Tuj-1 and BMP. Our results indicated that the colocalization of Tuj-1 and BMP expression was in the coculture system. Remarkably, Tuj-1 positive axons were accompanied by BMP expression cells. Higher magnification also revealed their co-localization, suggesting these differentiated ADSCs are functional. In contrast, DRG neuron axon was not wrapped by ADSCs, and no colocalization was found in co-culture system (Fig. 7A). Next, levels of 3 representative neurotrophic factors (NGF, BDNF, and GDNF) in culture supernatant of ADSCs-derived SCs were determined. ELISA experiment results showed that these ADSCs-derived SCs can produce the 3 factors, and their levels progressively elevated at induction time ranging from 1- to 3-weeks. Of note, the amount of 3 neurotrophic factors released from differentiated ADSCs at 3 weeks (96.4 ± 8.16 pg/ml for NGF; 82.44 ± 6.72 pg/ml for BDNF; and 78.58 ± 4.72 pg/ml GDNF) was significantly higher than at 1 (39.8 ± 4.88 pg/ml for NGF; 32.5 ± 4.83 pg/ml for BDNF; and 27.5 ± 2.67 pg/ml for GDNF) and 2 weeks (63.16 ± 6.21 pg/ml for NGF; 51.3 ± 4.56 pg/ml for BDNF; and 56.8 ± 6.06 pg/ml for GDNF). For normal ADSCs, the amount of 3 growth factor were 6.1 ±

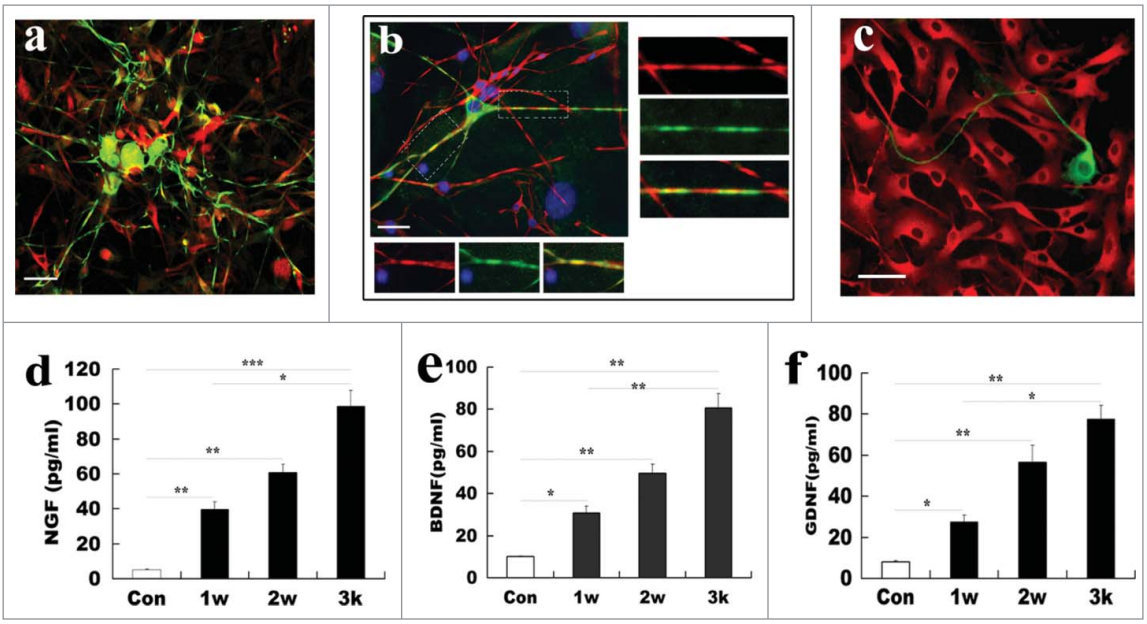

Figure 7. Functional assays of SCs derived from ADSCs. (A) Representative micrographs illustrated myelination formation in ADSC-derived SCs with DRG neurons. Notably, co-culture of DRG neurons (green for Tuj-1) with ADSCs-derived SCs (red for MBP) for 12 days, differentiated ADSCs processes were aligned to the neuronal axons, and even were wrapped at certain segments. (B) Myelin-formation was assayed in differentiated ADSCs and DRG neuron at low density. (C) ADSCs (red for CD90) do not form myelination with DRG neuron (green for Tuj-1). (D, E, F) Measurement of release of neurotrophic factors in the differentiated ADSCs at indicated induction time. All data are reported as mean ± SEM. $^{*}p<0.05$ compared with the relevant controls; $^{**}p<0.01$; and $^{**}p<0.001$. Scale bars = 200 μm.

0.45 pg/ml, 10.1 ± 0.63 pg/ml, and 8.56 ± 0.87 pg/ml, respectively (Fig. 7D, E and F) ($p<0.05$, $p<0.01$ and $p<0.001$ *vs* the corresponding control), suggesting that the ADSC-derived SCs gain the wild SC characteristic of release of growth factors.

Discussion

Currently, peripheral nerve injuries (PNI) are usually treated by surgically autologous SC transplantation or nerve graft. However, the outcomes of this therapeutic approach are not always satisfying mainly owing to sacrifice of healthy donor nerves, time consuming of expanding sufficient SCs and additional morbidity. For this reason, finding a viable cell-based therapy for PNI is essential. Lately, compelling studies show that apart from multipotency and strong proliferation, ADSCs have been an attractive cell source for neural regeneration, mainly due to certain unique advantages (ease of harvest, high proliferation rates for ex vivo expansion, no ethical and immune concerns, and lower tumorigenesis) compared with other types of stem cells.[26,28,29-31] To date, although there have been some successful methods of reprogramming ADSCs to SCs, the concerns including the long-term stability of these cells, differentiation efficiency, and functionality are largely unknown. For instance, following withdrawal of induction condition, some ADSCs-derived SCs very rapidly revert to stem cell morphology and phenotype, and significantly reduce growth factor expression as genuine SCs.[32] Therefore, these limit their clinical translatability into a peripheral nerve lesion.

In this study, we develop and optimize an induction system of ADSCs into SCs. Before differentiation, we confirmed that ADSCs from rat adipose tissue express characteristic MSC markers CD44, CD90, and CD29. Also, a fraction of these cells possessed a multipotency and stem-ness as a result of adipocytic, chondrogenic and osteogenic differentiation. Within the differentiation process, these differentiated cells showed a dramatic morphological change from fibroblast-like to spindle in shape. Moreover, the biochemical and phenotypic analysis by immunostaining, RT-PCR and western blotting revealed that these converted cells constitutively express GFAP and S100 under the special induction system, indicating these cells have acquired SC phenotype. In addition, the converted ADSCs can maintain high proliferative capacity after being passaged for culture. More importantly, these differentiated cells can form myelin when co-cultured with DRG neurons. Meanwhile, they can release NGF, BDNF and GDNF at time-dependent manner. These findings probably support our idea that the optimized induction method can effectively convert ADSCs into SC-like cells with morphological and functional attributes.

For the induction system, apart from the delivery of traditional induction factors, such as bFGF, forskolin, RA, and BME, we supplemented OECCM and SB as 2 important components in our induction system. The mixture of traditional cytokines was confirmed to induce SC differentiation, survival, and proliferation.[33-35] To maintain a SC phenotype *in vitro*, the combined multiple growth factors, such as NGF, BDNF, GGF, bFGF, PDGF, GDNF ect., seemed requisite.[36] Herein, OECCM was used to induce ADSC differentiation since OECs are capable of synthesising and secreting numerous growth factors such as NGF, BDNF, NT-3/4, GDNF, and neurturin, and extracellular adhesion molecules including fibronectin, laminin, tenascin, and NACM.[37-39] The unique property of OECs may exert a crucial role in direct conversion of ADSCs into SCs and further maintenance of SC phenotype. In our optimizing induction method, we found that the involvement of OECs indeed significantly improved the ADSC transdifferentiation efficiency as demonstrated by the morphology change and immunostaining

in presence or absence of OECCM. In Figure 4C and Figure 5C, the presence of OECCM remarkably promotes ADSC transdifferentiation when compared with the absence of OECCM, indicating that OECCM play a crucial role in conversion procedure. In addition, these ADSCs-derived SCs are stable and capable of forming myelin with DRG neuronal axons *in vitro* albeit shifting in the non-induction condition. This is consistent with a previous study that OECCM can promote differentiation of MSCs and spermatogonial stem cells into desired type of cells.[40,41] Therefore the possible underlying mechanism of OECs participation in inducing ADSCs to SCs is associated with the secretion of these growth factors and cell adhesion molecules. In addition, SB431542, a small molecule inhibitor of the TGF-β/activin/Nodal pathway, is actively involved in cytokine-mediated cell proliferation and differentiation.[42,43] Therefore, blockade of TGF-β signaling can potentiate conversion of mesenchymal stem cells into neural cells. It has been reported that TGF-β makes an important contribution to the decrease of neurogenesis in the aging brain.[44,45] Significantly, SB regulates intrinsic differentiation-related transcripts including epigenetic effectors associated with mesenchymal cells.[46] On the basis of our present results in combination with the previous reports, we speculated that the 2 components may play pivotal roles in neural conversion of ADSCs and maintenance of differentiated SC type.

Overall, this results presented here showed that we successfully induced the differentiation of ADSCs to SC-like cells. The differentiated cells acquire morphology and functionality similar to genuine SCs. The direct conversion of ADSCs to SCs using OECCM and SB combined with several factors without involvement of exogenous gene transfer is essential for shortening differentiation procedure and improving safety for future clinical application. Of unusual significance, our protocol for generation of functional SCs provide a novel, autologous cell replacement strategy to generate mature and phenotype stable SCs from patient for treatment of PNI and neural degenerative diseases.

Materials and methods

Cell culture

All experiments on animals were approved by the Animal Experimentation Ethics Committee of the National Academy of Science and implemented according to the guidelines established by The Ministry of Health of China. Primary of ADSCs were isolated from groin adipose tissue of 1.5-month-old SD rats according to the procedure described previously.[47] Briefly, the adipose tissue was carefully dissected, fully washed with ice-cold HBSS without Ca^{2+} and Mg^{2+}, and minced before transfer in 0.1% collagenase type I. After shaking at enzymatic digestion solution for 50 min at 37°C, the equal volume of DMEM containing 10% FCS was added. Thereafter, mechanical dissociation and centrifugation were further conducted to eliminate floating adipocytes. To harvest single cell suspension, the cell suspension was filtered with 60 nylon mesh. Finally, the cells were seeded into 60mm Petri dishes at a density of 1×10^4 cells /cm^2, and maintained at 37°C in a humidified 5% CO_2 incubator. Twelve hours later, the residual non-adherent cells were exterminated by washing with PBS and changing the medium. Of note, when ADSCs were reached 85% confluency, cell purification was implemented by flow cytometry sorting.

For harvesting OECCM, OECs were prepared according to the method descried previously.[48] After 7–10 d of culture, the medium was changed with DMEM/F12 containing 1% G5 supplement. The OECs were maintained for another 12 h at normal culture condition for condition culture medium.

As for neuron cultures, primary cultures of dorsal ganglion neurons were prepared from embryonic 12-day rats according to the procedure as described previously by Yang et al.[49] Briefly, the spinal cords with dorsal ganglion neurons were dissected and washed with ice-cold HBSS. Following removal of spinal cords, dorsal ganglion tissue was trypsinized with 2 mL of 0.125 % (w/v) trypsin at 37°C for 25 min before mechanical trituration. The dissociated cells were then collected by centrifugation and diluted to an approximate density of 2×10^5 cells/cm^2 with Neurobasal medium supplemented with 2 % B27, and plated into either 35-mm Petri dishes coated with poly-l-lysine (PLL). Cultures were maintained in an incubator at 37°C in a humidified atmosphere of 5% CO_2. The cultures were maintained and prepared for further experiments.

Preparation of olfactory ensheathing cell conditioned medium

The supernatant of subcultured OECs grown in DMEM/F12 containing G5 supplement was collected every day. One week later, these collected were mixed, centrifuged, and then filtered with a sterile 0.45 μm filter to exterminate cell debris. Finally these media were subdivided and kept at −80°C until used.

Flow cytometry

Briefly, the subcultured ADSCs were trypsinized with 0.125% Trypsin and 0.02% EDTA, collected and washed twice in ice-cold PBS. Single cell suspension was achieved by gentle triturating and filtering through 60 μm nylon mesh before analysis. Subsequently cells were spun down, resuspended and incubated simultaneously with 10 μl CD44 antibody directly conjugated to Alexa-488 and CD31 conjugated to 594 (0.25 μg/ml) for 1 h under constant rotation at RT and washed 3 times with PBS before flow cytometry analysis. Of note, before sorting, the system was fluxed for 10 min with ethanol 70 % to reduce contamination. Cells were centrifuged immediately after the sorting (1224×g for 5 min) and re-suspended in sterile growth medium for further culture.

Identification of ADSCs multipotency

To confirm the cultured ADSCs multipotency, passages 2 ADSCs after purification were seeded on 35 mm dishes for adipogenesis, chondrogenesis, and osteogenesis. Briefly, when cell confluency reached 80%, cell media were changed with adipogenic, chondrogenic, and osteogenic induction medium, respectively. The composition of these induction media were as described previously.[32] Of note, the culture medium was refreshed once every 3 d. After 21 days, cells were fixed with 4% paraformaldehyde for 25 min, washed 3 times with 0.01M

PBS, and stained with their respective dye solutions: Oil red O for the staining of fat droplets generated from ADSCs, Toluidine blue for chondrocytes, and Alizarin red S for ADSCs-derived from osteocytes. In parallel, each staining was performed on the normal cultured ADSCs as negative controls. Lastly, images were captured with Nikon's inverted microscope.

Induction of rat ADSCs into SC-like cells

Briefly, subcultured ADSCs at 2 passages were seeded at a density of 1×10^4 cells /cm^2 in 12-well plates. After 24 hours, different inductions were used as below: 1) OECCM + 20 μM SB + 5 μM forskolin + 5 μM RA + 5 μM BME + 10 ng/ml bFGF +5% FBS; 2) OECCM + 5 μM forskolin + 10 ng/ml bFGF +5% FBS; 3) OECCM + 20 μM SB + 5 μM forskolin + 5 μM RA + 10 ng/ml bFGF +5% FBS; 4) 20 μM SB + 5 μM forskolin + 5 μM RA + 5 μM BME + 10 ng/ml bFGF +5% FBS. The medium was refreshed every 3 days, and the cells were induced for 1, 2, and 3 weeks for various examinations.

MTT cell proliferation assay

For assessment of proliferative capacity of SCs derived from ADSCs at different passages, cells at passages 2, 3 and 4 were seeded at a density of approximately 10,000 cells per well in 96-well plates in DF/12 medium with 5% serum, respectively, and continually cultured for 1, 2, 3 and 4 d. At the indicated time points, 10μl of 50 mg/ml MTT (3-(4, 5-dimethylthiazolyl-2)-2,5-diphenyltetrazolium bromide) was added directly to per culture well and the cells were allowed to incubate for 4 h. After the incubation, the medium from each well was gently removed by aspiration and 200 μl Dimethylsulfoxide (DMSO) was added to each well followed by incubation and shaking for 10 min to dissolve the insoluble formazan. Culture plate with DMSO solutions were measured in a microplate reader at 570 nm (reference wavelength 630 nm) to determine the number of viable cells at 1, 2, 3 and 4 d after culture with MCM. All data presented in the present report were obtained from 3 independent experiments.

Total RNA extraction and reverse transcription PCR

Total RNA extraction, reverse transcription and PCR were performed using standard procedure according to manufacturer's instructions. GAPDH was used as internal control. The chosen target genes were as follows: GFAP, S100. The DNA primers used were as follows: S100, 5′-tgggcttccagagctttcta-3′, 5′-ttctttattgagggcaaccg-3′; GFAP, 5′-agggacaatctcacacagg-3′, 5′-gactcaaccttcctctcca-3′; GAPDH, 5′-gtttgtgatgggtgtgaacc-3′, 5′-tcttctgagtggcagtgatg-3′. The mRNA levels were quantified by SYBR green-based quantitative real-time PCR (Takara) using an ABI Prism 7900HT (Applied Biosystems, Foster City, CA USA), Results were confirmed by 3 independent experiments. Meanwhile, PCR products were visualized by electrophoresis on a 1.8% (W/V) gel stained with 0.5 μg/ml ethidium bromide and photographed under UV light. The gel image was captured in Gel Doc 1000 system (BioRad, Hercules, CA). Data analysis was performed according to described previously methods.[50]

Immunofluorescence staining

All cells from experimental group were fixed with 4% paraformaldehyde for 20 min, treated with 0.01% Triton X-100 (for verification of OEC identity, not treated with Triton X-100), and blocked with 3% normal donkey serum in 0.01 M PBS at room temperature (RT) for 30 min. The following primary antibodies were used: mouse anti-p75 (1:200), goat anti-GFAP (1:500), mouse anti-S100 (1:300), mouse anti-CD44 (1:300), rabbit anti-CD29 (1:400), and rabbit anti-CD90 (1:1000). Incubation of primary antibodies was performed at 4°C overnight. After washing thrice with PBS, cells were incubated with corresponding fluorescence conjugated secondary antibodies (Alexa Fluor 488-conjugated donkey anti-rabbit IgG antibody for Tuj-1, 1:400 dilution; Alexa Fluor 488-conjugated goat anti-mouse IgG for p75, 1:400 dilution; Alexa Fluor 594-conjugated donkey anti-goat IgG antibody for GFAP, 1:800 dilution; Alexa Fluor 594 donkey anti-mouse IgG antibody for S100, 1:500) for 1h at RT. Thereafter, counter staining using DAPI (2 μg/ml) at RT for 15 min was performed and fluorescence was evaluated using a confocal epifluorescence microscope (Leica). Immunofluorescence was performed in triplicate and representative images were captured.

Western-blot analysis

ADSCs induced with different conditions were lysed and the supernatant was collected for western blot analysis according to the protocol as described previously.[51] Following antibodies were used: GFAP and S100. β-actin was used as an internal control. After washes thrice in PBS, immunoblots were visualized using enhanced chemiluminescence. Densitometric analysis of bands was repeated for 4 times and IDV was calculated.

Myelination capacity evaluation of SC-like cells

To determine ADSCs-derived SC myelination capacity, the induced ADSCs for 3 weeks were subcultured at a density of 1×10^4 cells/cm^2 on the glass coverslips before being used for co-culture experiment. After 24–36 h, the cultured DRG neurons in Neurobasal plus 1% B27 for 3–5 d were detached, dissociated and re-seeded at a density of 1000 cells/cm^2 in ADSCs-derived SC culture. For control, normal dissociated ADSCs were used to co-culture. DRG neurons/ ADSCs-derived SCs co-cultures were maintained in Neurobasal plus 1% B27 and 10% FBS for 10 d and medium was changed every 3 d. After 10 days, the co-cultures were fixed in 4% paraformaldehyde in PBS for 15 min. Thereafter, the cells on coverslips were immunostained according to the abovementioned procedure. The used antibodies are Tuj-1 and MBP.

ELISA

To determine whether the ADSCs-derived SCs are functional as native SCs, the levels of neurotrophic factors BDNG, NGF, and GDNF were assessed by ELISA. Briefly, the supernatants of

ADSCs-derived SCs were collected, concentrated and were analyzed by ELISA kits for the neurotrophic factors according to the manufacturer's instructions. Of note, supernatants were should be filtered with 0.45 μm filter to remove cell debris before performance of assays. Each sample was assayed in triplicate, and final absorbance was determined at 450 nm with a synergy HT microplate spectrophotometer (BioTec)

Statistical analysis

One-way analysis of variance (ANOVA) was used to test the statistical significance of group differences. Unless otherwise indicated. Post-hoc pairwise comparisons between individual groups were made using the Tukey test. $^{*}P < 0.05$ significance level was used for statistical tests. All data are expressed as mean ± standard error of mean (SEM).

Disclosure of potential conflicts of interest

No potential conflicts of interest were disclosed.

Funding

This work was supported by the Natural Science Foundation of China (grant nos. 81372056, 81571208 and YJ2017001).The authors confirm that there has been no financial support for this research that could have influenced its outcome.

Authors' contributions

Hao Yang and Dahai Hu performed the microscopic and data analyses, conceived, designed, and coordinated the study, and wrote the manuscript. Xie Songtao performed the cell culture, immunofluorescence, cell differentiation and multipotency analysis. Lu Fan and Juntao Han performed RT-PCR. Ke Tao performed western-blot analysis and functional assessment of SCs derived from ADSCs. Taohong Wang designed part of experiments about neurite outgrowth. Alfred Simental participated in revising the manuscript.

ORCID

Hao Yang http://orcid.org/0000-0002-1144-0584

Reference

[1] Ciaramitaro P, Mondelli M, Logullo F, Grimaldi S, Battiston B, Sard A, Scarinzi C, Migliaretti G, Faccani G, Cocito D. Traumatic peripheral nerve injuries: Epidemiological findings, neuropathic pain and quality of life in 158 patients. J Peripher Nerv Syst 2010; 15(2):120-7; PMID:20626775; http://dx.doi.org/10.1111/j.1529-8027.2010.00260.x

[2] Jones S, Eisenberg HM, Jia X. Advances and future applications of augmented peripheral nerve regeneration. Int J Mol Sci 2016; 17(9): pii: E1494; http://dx.doi.org/10.3390/ijms17091494

[3] Wiberg M, Terenghi G. Will it be possible to produce peripheral nerves? Surg Technol Int 2003; 11:303-10; PMID:12931315

[4] Faroni A, Smith RJ, Lu L, Reid AJ. Human Schwann-like cells derived from adipose-derived mesenchymal stem cells rapidly de-differentiate in the absence of stimulating medium. Eur J Neurosci 2016; 43(3):417-30; PMID:26309136; http://dx.doi.org/10.1111/ejn.13055

[5] Pfister LA, Papaloïzos M, Merkle HP, Gander B. Nerve conduits and growth factor delivery in peripheral nerve repair. J Peripher Nerv Syst 2007; 12(2):65-82; PMID:17565531; http://dx.doi.org/10.1111/j.1529-8027.2007.00125.x

[6] Chen ZL, Yu WM, Strickland S. Peripheral regeneration. Annu Rev Neurosci 2007; 30:209-33

[7] Guénard V, Kleitman N, Morrissey TK, Bunge RP, Aebischer P. Syngeneic Schwann cells derived from adult nerves seeded in semipermeable guidance channels enhance peripheral nerve regeneration. J Neurosci 1992; 12(9):3310-20; PMID:1527582

[8] Ide C. Peripheral nerve regeneration. Neurosci Res 1996; 25 (2):101-21; PMID:8829147; http://dx.doi.org/10.1016/0168-0102(96)01042-5

[9] Morrissey TK, Kleitman N, Bunge RP. Isolation and functional characterization of Schwann cells derived from adult peripheral nerve. J Neurosci 1991; 11(8):2433-42; PMID:1869923

[10] Li Q, Ping P, Jiang H, Liu K. Nerve conduit filled with GDNF gene-modified Schwann cells enhances regeneration of the peripheral nerve. Microsurgery 2006; 26(2):116-21; PMID:16538638; http://dx.doi.org/10.1002/micr.20192

[11] Mosahebi A, Fuller P, Wiberg M, Terenghi G. Effect of allogeneic Schwann cell transplantation on peripheral nerve regeneration. Exp Neurol 2002; 173(2):213-23; PMID:11822885; http://dx.doi.org/10.1006/exnr.2001.7846

[12] Tohill MP, Mann DJ, Mantovani CM, Wiberg M, Terenghi G. Green fluorescent protein is a stable morphological marker for schwann cell transplants in bioengineered nerve conduits. Tissue Eng 2004; 10(9–10):1359-67; PMID:15588396; http://dx.doi.org/10.1089/ten.2004.10.1359

[13] Rutkowski GE, Miller CA, Jeftinija S, Mallapragada SK. Synergistic effects of micropatterned biodegradable conduits and Schwann cells on sciatic nerve regeneration. Neural Eng 2004; 1(3):151-7; http://dx.doi.org/10.1088/1741-2560/1/3/004

[14] Ziegler L, Grigoryan S, Yang IH, Thakor NV, Goldstein RS. Efficient generation of schwann cells from human embryonic stem cell-derived neurospheres. Stem Cell Rev 2011; 7(2):394-403; PMID:21052870; http://dx.doi.org/10.1007/s12015-010-9198-2

[15] Konig N, Trolle C, Kapuralin K, Adameyko I, Mitrecic D, Aldskogius H, Shortland PJ, Kozlova EN. Murine neural crest stem cells and embryonic stem cell-derived neuron precursors survive and differentiate after transplantation in a model of dorsal root avulsion. J Tissue Eng Regen Med 2014; 11(1):129-37.

[16] Kiel ME, Chen CP, Sadowski D. McKinnon RD Stem cell-derived therapeutic myelin repair requires 7% cell replacement. Stem Cells 2008; 26(9):2229-36; PMID:18635868; http://dx.doi.org/10.1634/stemcells.2008-0218

[17] Cui L, Jiang J, Wei L, Zhou X, Fraser JL, Snider BJ, Yu SP. Transplantation of embryonic stem cells improves nerve repair and functional recovery after severe sciatic nerve axotomy in rats. Stem Cells 2008; 26(5):1356-65.

[18] Ikeda M, Uemura T, Takamatsu K, Okada M, Kazuki K, Tabata Y, Ikada Y, Nakamura H. Acceleration of peripheral nerve regeneration using nerve conduits in combination with induced pluripotent stem cell technology and a basic fibroblast growth factor drug delivery system. J Biomed Mater Res A 2014; 102(5):1370-8; PMID:23733515; http://dx.doi.org/10.1002/jbm.a.34816

[19] Ma MS, Boddeke E, Copray S. Pluripotent stem cells for Schwann cell engineering. Stem Cell Rev 2015; 11(2):205-18; PMID:25433863; http://dx.doi.org/10.1007/s12015-014-9577-1

[20] Dezawa M, Takahashi I, Esaki M, Takano M, Sawada H. Sciatic nerve regeneration in rats induced by transplantation of *in vitro* differentiated bone-marrow stromal cells. Eur J Neurosci 2001; 14(11):1771-6; PMID:11860471; http://dx.doi.org/10.1046/j.0953-816x.2001.01814.x

[21] Caddick J, Kingham PJ, Gardiner NJ, Wiberg M, Terenghi G. Phenotypic and functional characteristics of mesenchymal stem cells differentiated along a Schwann cell lineage. Glia 2006; 54:840-9; PMID:16977603; http://dx.doi.org/10.1002/glia.20421

[22] Shimizu S, Kitada M, Ishikawa H, Itokazu Y, Wakao S. Dezawa M Peripheral nerve regeneration by the *in vitro* differentiated-human bone marrow stromal cells with Schwann cell property. Biochem Biophys Res Commun 2007; 359(4):915-20; PMID:17573041; http://dx.doi.org/10.1016/j.bbrc.2007.05.212

[23] Akiyama Y, Radtke C, Kocsis JD. Remyelination of the rat spinal cord by transplantation of identified bone marrow stromal cells. J Neurosci 2002; 22:6623-30; PMID:12151541

[24] Hou SY, Zhang HY, Quan DP, Liu XL, Zhu JK. Tissue-engineered peripheral nerve grafting by differentiated bone marrow stromal cells. Neurosci 2006; 140(1):101-10; http://dx.doi.org/10.1016/j.neuroscience.2006.01.066

[25] Kingham PJ, Kalbermatten DF, Mahay D, Armstrong SJ, Wiberg M, Terenghi G. Adipose-derived stem cells differentiate into a Schwann cell phenotype and promote neurite outgrowth *in vitro*. Exp Neurol 2007; 207(2):267-74; PMID:17761164; http://dx.doi.org/10.1016/j.expneurol.2007.06.029

[26] Liu Y Zhang Z, Qin Y, Wu H, Lv Q, Chen X, Deng W. A new method for Schwann-like cell differentiation of adipose derived stem cells. Neurosci Lett 2013; 551:79-83; PMID:23880021; http://dx.doi.org/10.1016/j.neulet.2013.07.012

[27] Zuk PA, Zhu M, Mizuno H, Huang J, Futrell JW, Katz AJ, Benhaim P, Lorenz HP, Hedrick MH. Multilineage cells from human adipose tissue: implications for cell-based therapies. Tissue Eng 2001; 7 (2):211-28; PMID:11304456; http://dx.doi.org/10.1089/107632701300062859

[28] Xu Y, Liu L, Li Y, Zhou C, Xiong F, Liu Z, Gu R, Hou X, Zhang C. Myelin-forming ability of Schwann cell-like cells induced from rat adipose-derived stem cells *in vitro*. Brain Res 2008; 1239:49-55; PMID:18804456; http://dx.doi.org/10.1016/j.brainres.2008.08.088

[29] Lo Furno D, Mannino G, Cardile V, Parenti R, Giuffrida R. Potential therapeutic applications of adipose-derived mesenchymal stem cells. Stem Cells Dev 2016. [Epub ahead of print]

[30] Harasymiak-Krzyżanowska I, Niedojadło A, Karwat J, Kotuła L, Gil-Kulik P, Sawiuk M, Kocki J. Adipose tissue-derived stem cells show considerable promise for regenerative medicine applications. Cell Mol Biol Lett 2013; 18(4):479-93; PMID:23949841; http://dx.doi.org/10.2478/s11658-013-0101-4

[31] Konno M, Hamabe A, Hasegawa S, Ogawa H, Fukusumi T, Nishikawa S, Ohta K, Kano Y, Ozaki M, Noguchi Y, et al. Adipose-derived mesenchymal stem cells and regenerative medicine. Dev Growth Differ 2013; 55(3):309-18; PMID:23452121; http://dx.doi.org/10.1111/dgd.12049

[32] Faroni A, Smith RJ, Lu L, Reid AJ. Human Schwann-like cells derived from adipose-derived mesenchymal stem cells rapidly de-differentiate in the absence of stimulating medium. Eur J Neurosci 2016; 43(3):417-30; PMID:26309136; http://dx.doi.org/10.1111/ejn.13055

[33] Liao D, Gong P, Li X, Tan Z, Yuan Q. Co-culture with Schwann cells is an effective way for adipose-derived stem cells neural transdifferentiation. Arch Med Sci 2010; 6(2):145-51; PMID:22371738; http://dx.doi.org/10.5114/aoms.2010.13885

[34] Davis JB, Stroobant P. Platelet-derived growth factors and fibroblast growth factors are mitogens for rat Schwann cells. J Cell Biol 1990; 110 (4):1353-60; PMID:2157720; http://dx.doi.org/10.1083/jcb.110.4.1353

[35] Kim HA, Ratner N, Roberts TM, Stiles CD. Schwann cell proliferative responses to cAMP and Nf1 are mediated by cyclin D1. J Neurosci 2001; 21(4):1110-6; PMID:11160381

[36] Shea GK, Tsui AY, Chan YS, Shum DK. Bone marrow-derived Schwann cells achieve fate commitment–a prerequisite for remyelination therapy. Exp Neurol 2010; 224(2):448-58; PMID:20483356; http://dx.doi.org/10.1016/j.expneurol.2010.05.005

[37] Ramon-Cueto A, Cordero MI, Santos-Benito FF, Avila J. Functional recovery of paraplegic rats and motor axon regeneration in their spinal cords by olfactory ensheathing glia. Neuron 2000; 25(2):425-35; PMID:10719896; http://dx.doi.org/10.1016/S0896-6273(00)80905-8

[38] Franceschini IA, Barnett SC. Low-affinity NGF-receptor and E-N-CAM expression define two types of olfactory nerve ensheathing cells that share a common lineage. Dev Biol 1996; 173(1):327-43; PMID:8575633; http://dx.doi.org/10.1006/dbio.1996.0027

[39] Woodhall E, West AK, Chuah MI. Cultured olfactory ensheathing cells express nerve growth factor, brain-derived neuro-trophic factor, glia cell line-derived neurotrophic factor and their receptors. Brain Res Mol Brain Res 2001; 88(1–2):203-13; PMID:11295250; http://dx.doi.org/10.1016/S0169-328X(01)00044-4

[40] Xie ST, Lu F, Zhang XJ, Shen Q, He Z, Gao WQ, Hu DH, Yang H. Retinoic acid and human olfactory ensheathing cells cooperate to promote neural induction from human bone marrow stromal stem cells. Neuromolecular Med 2013; 15(2):252-64; PMID:23288654; http://dx.doi.org/10.1007/s12017-012-8215-9

[41] Yang H, Liu Y, Hai Y, Guo Y, Yang S, Li Z, Gao WQ, He Z. Efficient conversion of spermatogonial stem cells to phenotypic and functional dopaminergic neurons via the PI3K/Akt and P21/Smurf2/Nolz1 pathway. Mol Neurobiol 2015; 52(3):1654-69; PMID:25373443; http://dx.doi.org/10.1007/s12035-014-8966-4

[42] Patani R, Compston A, Puddifoot CA, Wyllie DJ, Hardingham GE, Allen ND, Chandran S. Activin/Nodal inhibition alone accelerates highly efficient neural conversion from human embryonic stem cells and imposes a caudal positional identity. PLoS One 2009; 4(10): e7327; PMID:19806200; http://dx.doi.org/10.1371/journal.pone.0007327

[43] Chambers SM, Fasano CA, Papapetrou EP, Tomishima M, Sadelain M, Studer L. Highly efficient neural conversion of human ES and iPS cells by dual inhibition of SMAD signaling. Nat Biotechnol 2009; 27(3):275-80; PMID:19252484; http://dx.doi.org/10.1038/nbt.1529

[44] Marschallinger J, Krampert M, Couillard-Despres S, Heuchel R, Bogdahn U, Aigner L. Age-dependent and differential effects of Smad7-DeltaEx1 on neural progenitor cell proliferation and on neurogenesis. Exp Gerontol 2014; 57:149-54; PMID:24862634; http://dx.doi.org/10.1016/j.exger.2014.05.011

[45] Pineda JR, Daynac M, Chicheportiche A, Cebrian-Silla A, Sii Felice K, Garcia-Verdugo JM, Boussin FD, Mouthon MA. Vascular-derived TGF-beta increases in the stem cell niche and perturbs neurogenesis during aging and following irradiation in the adult mouse brain. EMBO Mol Med 2013; 5(4):548-62; PMID:23526803; http://dx.doi.org/10.1002/emmm.201202197

[46] Kumar P, Naumann U, Aigner L, Wischhusen J, Beier CP, Beier D. Impaired TGF-β induced growth inhibition contributes to the increased proliferation rate of neural stem cells harboring mutant p53. Am J Cancer Res 2015; 5(11):3436-45; PMID:26807323

[47] Huang YC, Ning H, Shindel AW, Fandel TM, Lin G, Harraz AM, Lue TF, Lin CS. The effect of intracavernous injection of adipose tissue-derived stem cells on hyperlipidemia-associated erectile dysfunction in a rat model. J Sex Med 2010; 7(4 Pt 1):1391-400; PMID:20141586; http://dx.doi.org/10.1111/j.1743-6109.2009.01697.x

[48] Ramón-Cueto A1, Cordero MI, Santos-Benito FF, Avila J. Functional recovery of paraplegic rats and motor axon regeneration in their spinal cords by olfactory ensheathing glia. Neuron 2000; 25(2):425-35; PMID:10719896; http://dx.doi.org/10.1016/S0896-6273(00)80905-8

[49] Yang H, Cong R, Na L, Ju G, You SW. Long-term primary culture of highly-pure rat embryonic hippocampal neurons of low-density. Neurochem Res 2010; 35(9):1333-42; PMID:20503070; http://dx.doi.org/10.1007/s11064-010-0189-0

[50] Hao DJ, Liu C, Zhang L, Chen B, Zhang Q, Zhang R, An J, Zhao J, Wu M, Wang Y, Simental A, He B, Yang H. Lipopolysaccharide and Curcumin Co-Stimulation potentiates olfactory ensheathing cell phagocytosis via enhancing their activation. Neurotherapeutics 2016 [Epub ahead of print]; PMID:27743319

[51] He BR, Xie ST, Wu MM, Hao DJ, Yang H. Phagocytic removal of neuronal debris by olfactory ensheathing cells enhances neuronal survival and neurite outgrowth via p38MAPK activity. Mol Neurobiol 2014; 49(3):1501-12; PMID:24258406; http://dx.doi.org/10.1007/s12035-013-8588-2